C. Barile et alii, Frattura ed Integrità Strutturale, 30 (2014) 211-219; DOI: 10.3221/IGF-ESIS.30.27

Focussed on: Fracture and Structural Integrity related Issues

Considerations on the choice of experimental parameters in residual stress measurements by hole-drilling and ESPI

C. Barile, C. Casavola, G. Pappalettera, C. Pappalettere
Dipartimento di Meccanica, Matematica e Management, Politecnico di Bari, viale Japigia 182, Bari, Italy
claudia.barile@poliba.it

ABSTRACT. Residual stresses occur in many manufactured structures and components. Great number of investigations have been carried out to study this phenomenon. Over the years, different techniques have been developed to measure residual stresses; nowadays the combination of Hole Drilling method (HD) with Electronic Speckle Pattern Interferometry (ESPI) has encountered great interest. The use of a high sensitivity optical technique instead of the strain gage rosette has the advantage to provide full field information without any contact with the sample by consequently reducing the cost and the time required for the measurement. The accuracy of the measurement, however, is influenced by the proper choice of several parameters: geometrical, analysis and experimental. In this paper, in particular, the effects of some of those parameters are investigated: misknowledgment in illumination and detection angles, the influence of the relative angle between the sensitivity vector of the system and the principal stress directions, the extension of the area of analysis and the adopted drilling rotation speed. In conclusion indications are provided to the scope of optimizing the measurement process together with the identification of the major sources of errors that can arise during the measuring and the analysis stages.

KEYWORDS. Residual stress; Electronic Speckle Pattern Interferometry (ESPI); Hole Drilling Method (HD); Process parameters; Titanium grade 5.

INTRODUCTION

The stress field existing in some materials without application of an external source of stress, such as loads or thermal gradients, is known as residual stress. These residual stresses are generated in almost all manufacturing processes such as machining, grinding, forming, rolling, casting, forging, welding, heat treatment, etc. or may occur during the life of structures.

The hole drilling method is one of the most widely used techniques for measuring residual stresses [1, 2]. This technique consists in the localized removal of stressed material and in measuring the strain field consequent to the relieved stresses. The hole drilling method using strain gauge rosettes [3, 4] is a consolidated approach for stress determination and it follows the ASTM test standard [5]. Even though strain gauges are usually used to measure these displacements, they have some disadvantages: the specimen surface has to be flat and smooth so that the rosettes can be attached, the surface of the material has to be accurately prepared, the hole has to be drilled exactly in the center of the rosette in order to avoid eccentricity errors, and time and costs associated with installing rosettes are consistent. Furthermore the amount of available data is limited: for each measurement, only three discrete readings are available (six in the case of some special rosettes), just sufficient to fully characterize the in-plane residual stresses.

The difficulties connected with the use of strain gauges could be promisingly overcame by using optical techniques [6]. During the past years, in fact, different approaches were explored for implementing hole drilling with optical methods. Several techniques can be used to generate fringe patterns, from which the local displacements, in the neighborhood of the hole, can be calculated. The use of moiré interferometry for residual stresses determination was investigated in many situations since McDonach et al. [7] and Martínez et al. [8]. However, bonding a grating can also be time consuming. The feasibility of using holographic interferometry was shown by Antonov [9]. Hung et al. [10] have used shearography in conjunction with a small ball indentation instead of a hole and also a phase shift shearography [11] was adopted. Also the possibility to release residual stresses by using local heat treatment, as in [12], was used by Pechersky et al. [13] combined with digital speckle pattern interferometry (DSPI). Instead Zhang [14] has investigated the practicability of the combination between DSPI and hole drilling. Electronic Speckle Pattern Interferometry (ESPI) which is an optical method based upon the speckle effect [15] has been increasingly used in the last decades. ESPI was successfully used to measure displacement field in anisotropic specimen made by selective laser melting [16-18], or orthotropic materials [19] as laminated wood [20] but also in combination with hole drilling method to evaluate the residual stress relieving [21] avoiding rigid-body motions [22].
In this paper the advantages of using ESPI technique in contrast to the classical method are underlined. Moreover all the parameters connected with the adoption of the ESPI technique that can be considered as a source of errors are analyzed and discussed. In defining the set-up it is necessary to have a good control of all the geometrical parameters involved, such as the angles that define the illumination and detection directions. If their values are not accurately evaluated this introduces an error in the determination of the displacement field which introduces an error in the calculation of the stress field [23]. Another factor that must be taken into account is that, in ESPI, displacement are measured along the sensitivity vector. In this paper the influence of the relative angle between the sensitivity direction and the principal stress is evaluated. Another important factor is the choice of the drilling rotation speed. Rotation speed, in fact, can affect the heat input to the material during the drilling process modifying the plasticization zone and it can affect the dimension of the drilling chips, introducing problems connected with the choice of the internal radius of analysis area [24, 25]. Also the combination of these effects [26, 27] must be taken adequately into account if high accuracy measurements are required.

CLASSIFICATION OF SOME POSSIBLE SOURCES OF ERRORS IN ESPI-HDM

In this section the entire measurement system including ESPI and hole-drilling equipment will be described as well as the list of potential sources of errors connected with the system, the analysis technique and the hole drilling process. Also the magnitude of the potential errors introduced will be estimated.

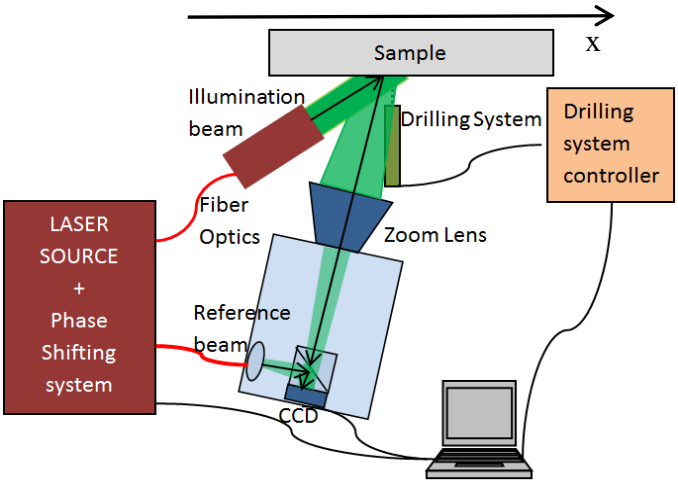

Figure 1: Experimental set-up for ESPI+HDM measurements.

The ESPI hole-drilling measurement system used in this work is schematically reported in Fig. 1.
A beam from a DPSS laser source is splitted into two beams and focused into two monomode optical fibers. One beam is collimated and illuminates the sample, while the second beam passes through a phase shifting piezoelectric system and then it goes to the CCD camera where interferes with the light diffused by the optically rough surface of the specimen.

Initial phase and final phase are evaluated by the four-step phase shifting technique, once the initial and the final phase are determined it is possible to calculate the amount of displacement of each point into the analysis area. The holes are drilled by means of a high speed turbine, electronically regulated; it is mounted on a precision travel stage in order to allow accurate positioning of the drilling device. Experimental measurements were performed on a titanium grade 5 specimens.

Geometrical parameters

The geometry and mutual position of laser, CCD and specimen should be accurately defined to correctly measure the displacement map. The *xyz* reference system of the specimen and the *x'y'z'* reference system of the CCD camera are considered as shown in Fig. 2. To exactly calculate strains from measured displacements, it is necessary to evaluate the pixel size along *x* and *y* directions, this means that the angles of CCD camera with respect to the specimen reference system *xyz* are needed. The α_2 angle defines the *x* axis and the *x'* axis; the β_2 angle defines the *z* axis and the *z'* axis; the γ_2 angle defines the *y* axis and the *y'* axis.

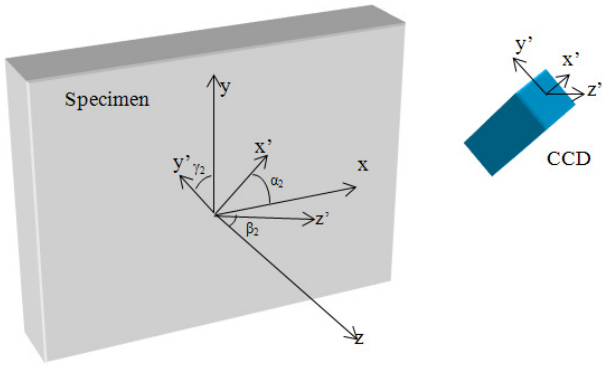

Figure 2: Schematic of the geometrical set-up with the CCD camera and the specimen.

Moreover, to calculate strains from measured displacements, it is necessary to know the phase changing of the pattern, detected during tests, and the sensitivity of the optical set up that depends on the geometry of the illumination system. Due to the cylindrical symmetry of the illumination beam around the propagation direction of the laser, only two angles are necessary in this case to relate the specimen reference system and the illumination reference system. Being *x"y"z"* the illumination beam reference system, the α_1 angle defines the *x* axis and the *x"* axis, while the β_1 angle defines the *z* axis and the *z"* axis. These geometric angles can be initially measured by a goniometer. The uncertainty in this measurement is estimated to be $\Delta=\pm 2°$ because of the difficulties to correctly positioning the goniometer inside the measurement system. In order to assess the influence in the geometrical parameters measuring of an error on the results in terms of measured stress, simple experimental tests were run. Rectangular cross section titanium specimen was subjected to three point bending load and induced stresses were measured as shown in Fig. 3.

The profile of the induced stresses was measured. The angle values were $\alpha_1=42.5°$; $\beta_1=0°$; $\alpha_2=24°$; $\beta_2=0°$; $\gamma_2=0°$. Then stress profile was recalculated by hypothesizing an error $\pm 2°$ on each of the considered angles and compared in order to detect the error on stress values $\Delta\sigma_{xx}$.

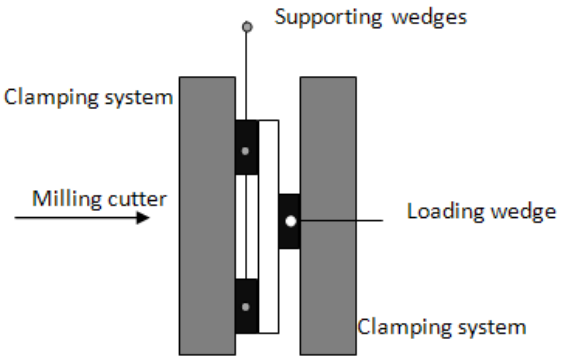

Figure 3: Top view of the three-point bending load frame.

It was found that a ±2° of the in-plane detection angle α_2 can introduce the higher error on the measured stress profile with respect to the other angles. Fig. 4 shows the effect of an error $\Delta\alpha_2=\pm 2°$ while in Tab. 1 are reported the numerical results and the effects in terms of percentage error on the calculated stress profile.

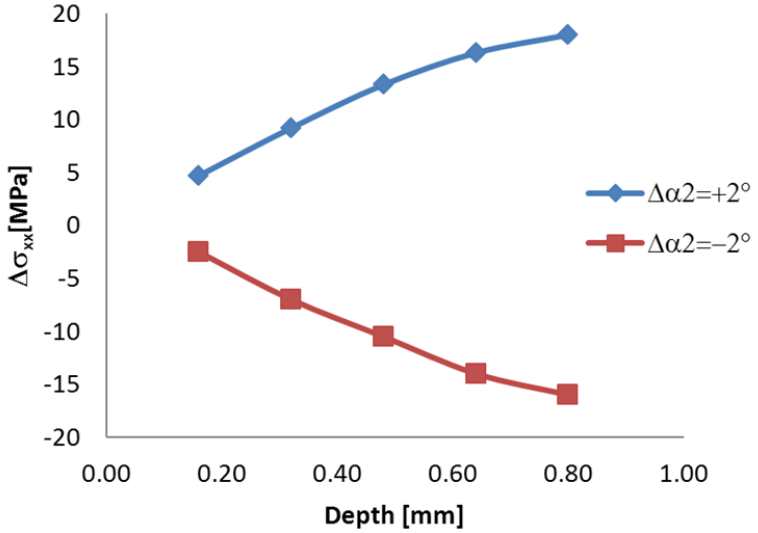

Figure 4: Differences in calculated stress in correspondence of an error of Δα2=+2° (rumble, blue dots) and $\Delta\alpha_2$=-2° (squared, red dots) with respect to the measured angle

Depth [mm]	σ_{xx} [MPa] (α_2=24°)	σ_{xx} [MPa] (α_2=22°)	σ_{xx} [MPa] (α_2=26°)	$\Delta\sigma_{xx}$ % ($\Delta\alpha_2$=-2°)	$\Delta\sigma_{xx}$ % ($\Delta\alpha_2$=+2°)
0.16	-393	-396	-389	0.6	1.2
0.32	-314	-321	-305	2.2	2.9
0.48	-268	-279	-255	3.9	5.0
0.80	-213	-229	-195	7.5	8.4

Table 1: Calculated stress σ_{xx} for measured α_2 = 24° and percentage errors for $\Delta\alpha_2=\pm 2°$.

Analysis area definition

The size of the analysis area can affect the results in terms of residual stresses (Fig. 5). If the radius of the inner circle is too small, error can arise due to the inclusion of some bad pixel in the analysis area due to some chips deposited near the edge of the hole. On the other side, if the outer radius is too large, a region of very small deformations is considered and this can lead to introduce an error especially in the case where low stresses have to be measured in material with high Young modulus.

In order to evaluate the influence of the analysis area, a bending stress state was induced on the specimen. The stress field was initially measured adopting the values of the inner radius (R_{int}) and the outer radius (R_{ext}) commonly used in this kind of experiments. This values are usually defined in terms of ratio with the radius of the drilled hole (R_{hole}), and it is common use to adopt $r_{int}=\frac{R_{int}}{R_{hole}}=2$. and $r_{ext}=\frac{R_{ext}}{R_{hole}}=4$ .n order to highlight the influence of r_{int} on the obtained stress values, a new calculation was performed by changing the inner radius ratio in the range $r_{int} \in [2,2.7]$ and keeping R_{ext} unchanged. Analogously, the outer radius ratio was changed in the range $r_{ext} \in [3,4.36]$ while keeping R_{int} constant. The upper value 4.36 of the r_{ext} range was limited by the image dimensions.

Tab. 2 reports the stress values for the default radius of r_{ext}=4 and the percentage change of stresses using different r_{ext}. Fig. 6 shows di difference in terms of stress profiles calculated with respect to the reference values r_{ext}=4.

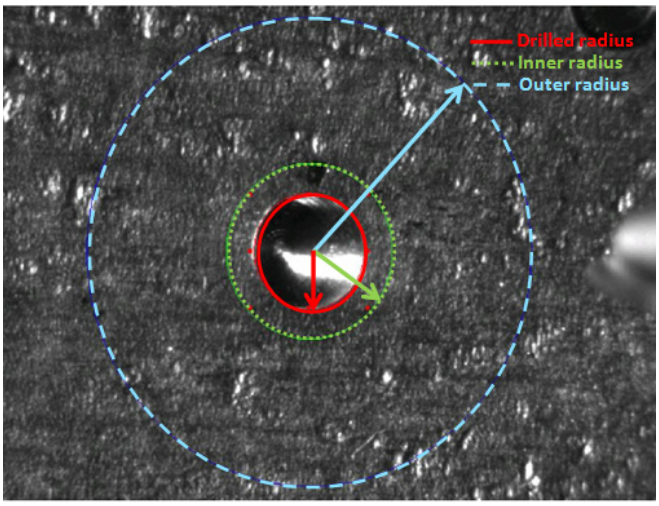

Figure 5: Screenshot of the area of analysis included between the outer circle (dashed line) and the inner circle (dotted line). The solid line identifies the drilled hole.

Depth [mm]	σ_{xx} [MPa] (r_{ext}=4)	σ_{xx} [MPa] (r_{ext}=3)	$\lvert\Delta\sigma_{xx}\,\%\rvert$ (Δr_{ext}=-1)	σ_{xx} [MPa] (r_{ext}=3.5)	$\lvert\Delta\sigma_{xx}\,\%\rvert$ (Δr_{ext}=-0.5)	σ_{xx} [MPa] (r_{ext}=4.36)	$\lvert\Delta\sigma_{xx}\,\%\rvert$ (Δr_{ext}=+0.358)
0.04	148	131	11.5	142	4.0	150	1.3
0.12	126	118	6.3	124	1.6	128	1.6
0.20	103	101	1.9	102	0.9	103	0.0
0.28	103	96	7	99	3.4	107	3.9
0.36	68	72	5.8	70	2.9	68	5.5

Table 2: Summary of the calculated stress for the default radius of r_{ext}=4 and the percentage change of stresses $\Delta\sigma_{xx}$ using different r_{ext}.

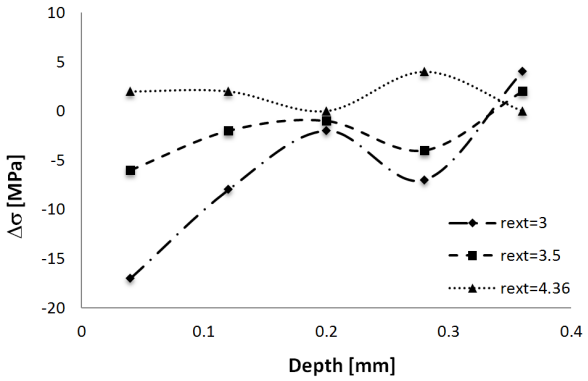

Figure 6: Plot of the difference in terms of measured stress at different depths. The difference are calculated for three different values of the external radius with respect to the reference value r_{ext}=4

It can be observed that increasing the external radius of analysis to the maximum value R_{ext} =3.48 mm (r_{ext}=4.36), which means an 8.95% of variation with respect to the default value, calculated stress at 0.36 mm depth changes about 5.5 %. Analogously, decreasing the external radius of analysis to the value R_{ext}=2.4 mm (r_{ext}=3), which means a 25% of variation with respect to the default value, the calculated stress at 0.36 mm depth changes about 5.8 %. From Fig. 5 it can also infer that the maximum difference (17 MPa) is obtained by using the smallest value of external radius in correspondence of the smallest depth, that is to say at about 11.5 % of variation. This attitude could be connected to the fact that reducing the

amount of data for the calculation of residual stress introduce a variation especially in the case when small amount of displacement need to be measured as it happen in the very first step.
A further investigation on analysis area was performed by keeping constant the radius ratio of the external circle of analysis r_{ext}=4 and by changing the value of r_{int} (Fig. 7). Tab. 3 summarizes the corresponding numerical stress values with the indication of the percentage variation with respect to the stresses calculated by using the default value r_{int}=2.

Depth [mm]	σ_{xx} [MPa] (r_{int}=2)	σ_{xx} [MPa] (r_{int}=1.25)	$\lvert\Delta\sigma_{xx}\,\%\rvert$ (Δr_{int}=-0.75)	σ_{xx} [MPa] (r_{int}=1.5)	$\lvert\Delta\sigma_{xx}\,\%\rvert$ (Δr_{int}=-0.5)	σ_{xx} [MPa] (r_{int}=2.5)	$\lvert\Delta\sigma_{xx}\,\%\rvert$ (Δr_{int}=+0.5)
0.04	148	159	7.4	148	0	146	1.3
0.12	126	121	3.9	122	3.2	135	7.1
0.20	103	85	17.4	94	8.7	115	11.6
0.28	103	104	9.7	107	3.8	99	3.9
0.36	68	56	17.6	62	8.8	73	7.3

Table 3: Summary of the calculated stress for the default radius of r_{int}=2 and the percentage change of stresses $\Delta\sigma_{xx}$ using different r_{int}.

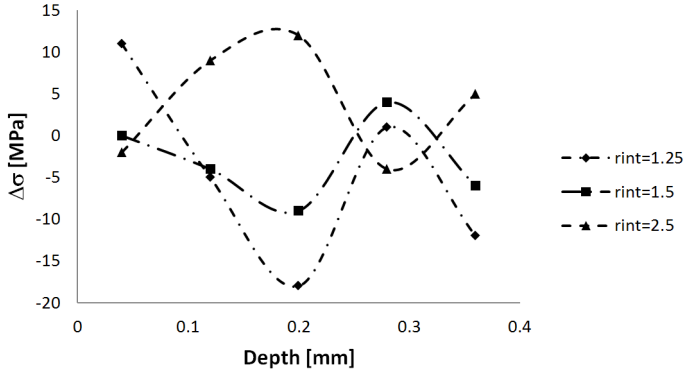

Figure 7: Plot of the difference in terms of measured stress at different depths. The difference are calculated for three different values of the internal radius with respect to the reference value r_{int}=2

It can be observed that by reducing the internal radius of analysis to the minimum value R_{int} =1 mm (r_{int}=1.25), which means a 37.5% of variation it is possible to observe a variation in the calculated stress up to 17.6 %. Analogously, by increasing the internal radius of analysis to the value R_{int}=2 mm (r_{int}=2.5), which means a 25% of variation with respect to the default value, the calculated stress shows a maximum variation of about 11.6 %. From Fig. 6 it is possible to infer that, in this case, the entity of the variation doesn't appear to be in some way connected to the depth. Variation stays still quite low if the r_{int}=1.5 ratio is used while the maximum difference (18 MPa) it is obtained by using the smallest value of the internal radius and this could be connected to the fact that by reducing to much the position of the inner circle of analysis, edge effects and bad quality pixel are introduced in the calculation so that an increment of the error can be found.

Sensitivity vector

It needs to be underlined that in the measurement system displayed in Fig. 1 the in-plane displacements consequent to the stress relaxation are measured only along the *x* direction. In this sense the system appears to be different respect to the strain gage rosette where each extensimeter grid measures strain along different directions. The measured amount of displacement depends on the angle between the relieved stress and the sensitivity vector. If one applies a perfect uniaxial load, as tensile or simple bending test, the stress field can be identified by the maximum principal stress σ_1 while the minimum principal stress can be put equal to 0. If measurements are executed with σ_1 direction overlapped to the sensitivity vector, the relieved strain is proportional to σ_1 according to the Hooke's law. On the other hand, if the sample is positioned inside the measurement system so that the σ_1 direction is perpendicular to the sensitivity vector, the relieved strain is proportional to $\nu\cdot\sigma_1$ according to the transversal contraction of the material. In view of these observations it appears interesting to understand how the accuracy of the measurement can be affected by the orientation of the principal

stresses with respect to the ESPI sensitivity direction. To this scope a specimen was bent in a four-points frame to obtain an uniaxial stress state with an applied stress σ_1=133 MPa and σ_2=0 MPa. Results can be summarized as it follows:

- in all cases the θ angle between the maximum principal stress and the *x* axis was correctly identified and with a small percentage error. It was found a value of θ=-0.45° for measurement in which the specimen is oriented with the maximum principal stress parallel to the *x* axis and θ=-0.24° when the specimen is oriented perpendicularly to the *x* axis;
- the measurement of the maximum principal stress is not significantly affected by the orientation of the specimen; the entity of the error is about 10 % and this is a value consistent with errors reported in other studies [28,29];
- concerning with the measurement of the minimum principal stress and in particular to its value along the thickness it was found that better results are obtained when the longitudinal axis of the specimen is oriented at 90° with respect to the *x* direction that is to say when the minimum stress is oriented along the sensitivity direction of the ESPI system (Tab. 4).

Specimen angle (°)	σ_2 ESPI (MPa)	σ_2 expected(MPa)	Δ (MPa)
0	13.2	2.3	11.0
90	5.7	2.3	3.4

Table 4: Results of the measurement of the minimum principal stress, σ_2, at 0.4 mm.

Results seem to be in contrast with the general theory that favors the overlapping of σ_1 with the sensitivity vector, but this attitude could be justified considering that the amplitude of load applied in all cases is large enough to be detected at all slopes. The limit condition could be reached decreasing the four-point bending load up to reduce at minimum the number of fringes in correspondence of different angle from the sensitivity vector.

Drilling speed

The effects of the drilling speed have also been analyzed. An electronic controlled drilling machine is used to drill the holes. Holes are drilled at three different velocities: 5000 rpm, 35000 rpm, 50000 rpm. The first and the last values represent, respectively, the minimum and the maximum rotation speed attainable by the drilling system. ESPI was used to detect the displacement map in correspondence of each drilling step. Also in this case specimen were loaded in a four-point bending frame in order to introduce a well-known stress field. As it can be inferred from Fig. 8 the average value of the measured stress state is coherent with the expected theoretical value and almost independent from the drilling speed. However data corresponding to lower speed appear more scattered than data recorded at the maximum speed. In fact the standard deviation for the measurement at 5K rpm is $St.Dev_{5K}$=26.6 MPa that is to say about 20 % of the expected value. This value decreases at 35K rpm being $St.Dev_{35K}$=8.8 MPa that is to say about 6 % of the nominal expected value and it reaches the minimum at 50K rpm where it is $St.Dev_{50K}$=3.9 MPa that is to say less than 3 % of the expected theoretical value. In other words the accuracy and the repeatability of the measurement diminishes by decreasing the rotation speed. This occurrence can be tracked back to the quality of the drilled hole, as reported in Fig. 9, left image refers to a hole drilled at 5000 rpm, middle image refers to a hole drilled at 35000 rpm and right image refers to a hole drilled at 50000 rpm. The quality of the hole profile appears to be compromised at lower speed.

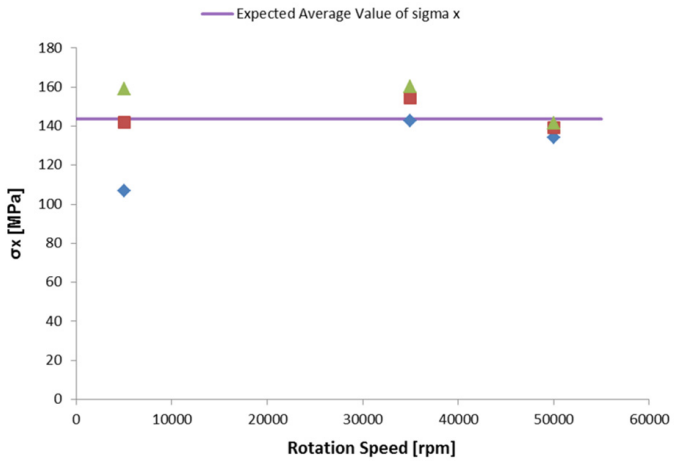

Figure 8: Plot of the measured stress at the different rotations speed of the cutter.

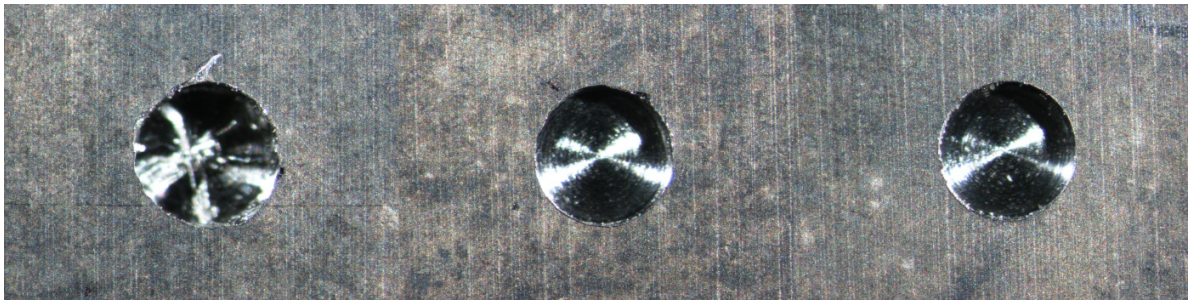

Figure 9: Image of the drilled holes obtained at the optical microscope 20x.

CONCLUSIONS

Hole-drilling method is one of the most adopted and reliable approach for measuring residual stress and it can takes advantages by its application in combination with ESPI because this can result in cheaper and faster measurements. However getting accurate results with this technique requires a good control over the many factors that can affect the final results. In this paper a review of some major sources of errors were presented and their effects were evaluated for the case of measurements on Ti Grade 5 sample. A good evaluation of the geometrical parameters it is relevant. In particular, for the adopted configuration, it is important to correctly determine the illumination angle. It was found that an error of ±2° on this parameter can introduce an error of about ±3.5 % on the final calculated stress. Also the positioning of the area of analysis is important, in some cases, due to geometrical constraints, this area need to be reduced however it should be taken into account that error of the order of 15 MPa could be introduced if the external radius is reduced too much especially in the very first steps. Similar results are obtained if the internal radius of analysis is changed too much with respect to the default value. Finally it should be reminded that the final quality of the drilled hole is a key factor in determining a good measurement. This is a goal which is strictly connected with the particular material under study, its machinability and the use of proper drilling material. However, final quality is also related with the proper choice of the drilling rotation speed. This parameter must be optimized as a function of the material under study. In this paper, in particular, effects of drilling rotation speed were studied on Ti grade 5. This is an interesting material to be studied in view of its very good strength-to-density ratio, and good corrosion resistance, properties that lead to an increasing demand of this material in aircraft industry [30]. It was found that much better quality is obtained by using higher velocity (50000 rpm), which is suggested therefore for measurements on this specific material. Care must be taken, however, to avoid that fine chips resulting from drilling operations, at this speed, stick to the material degrading the quality of the speckle fringe pattern and, as a consequence, the accuracy of the measurement itself.

REFERENCES

[1] Rendler, N.J., Vigness, I., Hole-drilling strain-gage method of measuring residual stresses, Exp. Mech., 6 (1966) 577-586.
[2] ASTM E387-92 Standard test method for determining residual stresses by the hole-drilling strain gage method. Annual book of ASTM standards, Philadelphia: American Society for Testing and Materials, 03.01 (1992) 747–753.
[3] Schajer, G.S., Roy, G., Flaman, M.T., Lu, J., Hole drilling and ring core methods, Lu J (ed) Handbook of measurement of residual stresses. Society for Experimental Mechanics, Bethel, (1996) 5–35.
[4] Schajer, G.S. Advances in hole-drilling residual stress measurements. Exp Mech., 50 (2009) 159-168.
[5] Standard test method for determining residual stresses by the hole-drilling strain-gage method standard E837-08. American Society for Testing and Materials, West Conshohocken, PA, (2008)
[6] Furgiuele, F.M., Pagnotta, L., Poggialini, A., Measuring residual stresses by hole drilling and coherent optics techniques: a numerical calibration, J. Eng. Mater. Technol., 113 (1991) 41–50.
[7] McDonach, A., McKelvie, J., MacKenzie, P.M., Walker, C.A., Improved moiré interferometry and applications in fracture mechanics, residual stresses and damage composites, Exp. Technol., 7 (1983) 20–24.
[8] Martínez, A., Rodríguez-Vera, R., Rayas, J. A., Puga, H. J., Fracture detection by grating moiré and in-plane ESPI techniques, Opt. Laser. Eng., 39 (5-6) (2003) 525–536.

[9] Antonov, A.A., Inspecting the level of residual stresses in welded joints by laser interferometry, Weld. Prod., 30 (1983) 29–31.
[10] Hung, Y.Y., Hovanesian, J.D., Fast detection of residual stress in an industrial environment by thermoplastic-based shearography. SEM Spring Conference on Experimental Mechanics, Albuquerque, USA, (1990) 769–775.
[11] Hung, M. Y. Y., Long, K. W., Wang J. Q., Measurement of residual stress by phase shift shearography, Opt. Laser. Eng., 27(1) (1997) 61–73.
[12] Barile, C., Casavola, C., Pappalettera, G., Pappalettere, C., Feasibility of Local Stress Relaxation by Laser Annealing and X-ray Measurement, Strain, 49(5) (2013) 393-398.
[13] Pechersky M.J., Miller R.F., Vikram C.S., Residual stress measurements with laser speckle correlation interferometry and local heat treating, Opt. Eng., 34 (1995) 2964–2971.
[14] Zhang J., Two-dimensional in-plane electronic speckle pattern interferometer and its application to residual stress determination, Opt. Eng., 37 (1998) 2402–2409.
[15] Cloud, G. L., Optical Methods of Engineering Analysis, Cambridge University Press, New York (1995).
[16] Barile, C., Casavola, C., Pappalettera, G., Pappalettere, C., Mechanical characterization of SLM specimens with speckle interferometry and numerical optimization, Exp. Applied Mech., of Conference Proceedings of the Society for Experimental Mechanics Series, Springer, NewYork, NY,USA, 6 (2011) 837–843.
[17] Barile, C., Casavola, C., Pappalettera, G., Pappalettere, C., Experimental and numerical characterization of sinterized materials with speckle interferometry and optimization methods, Proceedings of the 10th youth symposium on experimental solid mechanics (YSESM), Chemnitz, Germany, (2011) 35–36.
[18] Barile, C., Casavola, C., Pappalettera, G., Pappalettere, C., Mechanical characterization of SLM specimens with speckle interferometry and numerical optimization, Society for Experimental Mechanics - SEM Annual Conference and Exposition on Exp. and Applied Mech., 3 (2010) 2523-2529.
[19] Baldi, A., Full field methods and residual stress analysis in orthotropic material. I linear approach, Int. J. Solids Struct., 44 (25-26) (2007) 8229–8243.
[20] Barile, C., Casavola, C., Pappalettera, G., Pappalettere, C., Hybrid characterization of laminated wood with ESPI and optimization methods, Proceedings of the Society for Experimental Mechanics Series Conference, 3 (2013) 75–83.
[21] Sedivý, O., Krempaszky, C., Holý, S., Residual Stress Measurement by Electronic Speckle Pattern Interferometry, 5th Australasian Congress on Applied Mechanics, ACAM 2007, Brisbane, Australia (2007).
[22] Schajer, G. S., Steinzig, M., Full-field calculation of hole drilling residual stresses from electronic speckle pattern interferometry data, Exp. Mech., 45(6) (2005) 526-532.
[23] Barile, C., Casavola, C., Pappalettera, G., Pappalettere, C., Residual stress measurement by electronic speckle pattern interferometry: a study of the influence of geometrical parameters, Structural and Integrity in life - Integritet i vek konstrukcija, 11(3) (2011) 177-182.
[24] Barile, C., Casavola, C., Pappalettera, G., Pappalettere, C., Drilling speed effects on accuracy of HD residual stress measurements, In: Conference Proceedings of the Society for Experimental Mechanics Series, 8 (2014) 119-125.
[25] Barile, C., Casavola, C., Pappalettera, G., Pappalettere, C., Remarks on Residual Stress Measurement by Hole-Drilling and Electronic Speckle Pattern Interferometry, The Scientific World Journal, (2014).
[26] Steinzig, M., Ponslet, E., Residual stress measurement using the hole drilling method and laser speckle interferometry: part III, Exp. Techniques, 27(5) (2003) 45–48.
[27] Barile, C., Casavola, C., Pappalettera, G., Pappalettere, C., Analysis of the effects of process parameters in residual stress measurements on Titanium plates by HDM/ESPI, Measurement: Journal of the International Measurement Confederation, 48(1) (2014) 220-227.
[28] Steinzig, M., Takahashi, T., Residual stress measurement using the hole drilling method and laser speckle interferometry part IV: Measurement accuracy, Experimental Techniques, 27(6) (2003) 59-63.
[29] Viotti, M.R., Albertazzi Jr., A.G., Kapp, W., Experimental comparison between a portable DSPI device with diffractive optical element and a hole drilling strain gage combined system, Optics and Lasers in Engineering, 46(11) (2008) 835-841.
[30] Casavola, C., Lamberti, L., Pappalettere, C., Tattoli, F. A comprehensive numerical stress - Strain analysis of laser beam butt-welded titanium compared with austenitic steel joints, Journal of Strain Analysis for Engineering Design, 45(7) (2010) 535-554.